

REPORT DOCUMENTATION PAGE

Form Approved
OMB No. 0704-0188

Public reporting burden for this collection of information is estimated to average 1 hour per response, including the time for reviewing instructions, searching existing data sources, gathering and maintaining the data needed, and completing and reviewing the collection of information. Send comments regarding this burden estimate or any other aspect of this collection of information, including suggestions for reducing this burden, to Washington Headquarters Services, Directorate for Information Operations and Reports, 1215 Jefferson Davis Highway, Suite 1204, Arlington, VA 22202-4302, and to the Office of Management and Budget, Paperwork Reduction Project (0704-0188), Washington, DC 20503.

1. AGENCY USE ONLY (Leave Blank)	2. REPORT DATE 1 June 00	3. REPORT TYPE AND DATES COVERED Final Technical Report 1 July 97 to 30 April 00	
4. TITLE AND SUBTITLE Waveguide-Based Spatial Power Combiners		5. FUNDING NUMBERS DAAG55-97-1-0352	
6. AUTHORS Robert A. York			
7. PERFORMING ORGANIZATION NAME(S) AND ADDRESS(ES) Department of Electrical and Computer Engineering University of California, Santa Barbara Santa Barbara, CA 93106-9560		8. PERFORMING ORGANIZATION REPORT NUMBER	
9. SPONSORING / MONITORING AGENCY NAME(S) AND ADDRESS(ES) U.S. ARMY Research Office P.O. Box 12211 Research Triangle Park, NC 27709-2211		10. SPONSORING / MONITORING AGENCY REPORT NUMBER ARO 37559.1-EL	
11. SUPPLEMENTARY NOTES The views, opinions and/or findings contained in this report are those of the author(s) and should not be construed as an official Department of the Army position, policy or decision, unless so designated by other documentation.			
12a. DISTRIBUTION / AVAILABILITY STATEMENT Approved for public release; distribution unlimited		12b. DISTRIBUTION CODE	
13. ABSTRACT (Maximum 200 words) The objective of this program was to explore certain extensions of waveguide-based combiner systems in order to extend or enhance operating bandwidth and amplifier capacity. Oversized TEM-mode combiners were originally proposed which promise multi-octave bandwidths, and an enlarged cross-section compared with standard waveguide, which accommodates a larger number of amplifiers. During the program and in consultation with DARPA and ARO program managers, the program thrust was modified to include modeling and development of combiners at K-band, targeting existing commercial and military application demands. Significant progress was made in this effort, resulting in multiple demonstrations of combiner modules that could potentially challenge vacuum electronics in some applications. We have demonstrated a multi-octave 64-way passive combiner system using oversized coaxial waveguide. We also developed an oversized K-band (18-20GHz) combiner system that accommodates up to 24 amplifier circuits. In addition, we have developed a design methodology for creating optimum impedance tapers for the finline arrays used in this work.			
14. SUBJECT TERMS		15. NUMBER OF PAGES 13	
		16. PRICE CODE	
17. SECURITY CLASSIFICATION OF REPORT Unclassified	18. SECURITY CLASSIFICATION OF THIS PAGE Unclassified	19. SECURITY CLASSIFICATION OF ABSTRACT Unclassified	20. LIMITATION OF ABSTRACT UL

NSN 7540-01-280-5500

Standard Form 298 (Rev. 2-89)
Prescribed by ANSI Std. Z39-1
298-102

Final Technical Report

Title: Waveguide-Based Spatial Power Combiners

Contract Number: DAAG55-97-1-0352

Statement of Problem:

The objective of this program was to explore certain extensions of waveguide-based combiner systems in order to extend or enhance operating bandwidth and amplifier capacity. Oversized TEM-mode combiners were originally proposed which promise multi-octave bandwidths, and an enlarged cross-section compared with standard waveguide, which accommodates a larger number of amplifiers. During the program and in consultation with DARPA and ARO program managers, the program thrust was modified to include modeling and development of combiners at K-band, targeting existing commercial and military application demands.

Summary Accomplishments:

Significant progress was made in this effort, resulting in multiple demonstrations of combiner modules that could potentially challenge vacuum electronics in some applications. We have demonstrated a multi-octave 64-way passive combiner system using oversized coaxial waveguide. We also developed an oversized K-band (18-20GHz) combiner system that accommodates up to 24 amplifier circuits. In addition, we have developed a design methodology for creating optimum impedance tapers for the finline arrays used in this work.

List of Publications Resulting from this Work:

1. N.-S. Cheng, "Waveguide-Based Spatial Power Combiners", Ph.D. Dissertation (ECE Technical Report #99-08), Dept. of Electrical and Computer Engineering, University of California, Santa Barbara CA, 93106, June 1999.
2. P. Jia, L-Y Chen, N-S. Cheng, and R.A. York, "Design of Waveguide Finline arrays for Spatial Power Combining", to appear in *IEEE Trans. Microwave Theory Tech.*, 2000.
3. N.S. Cheng, L.Y. Chen, and R. A. York, "Waveguide-based Spatial Power Combiners," presented at *URSI National Radio Science Meeting*, (Boulder, CO), January 1999
4. R.A. York, "Spatial power combining", (Invited Paper), presented at *URSI General Assembly*, (Toronto, Canada), August 1999.
5. N.-S. Cheng and R. A. York, "Analysis and Design of tapered Finline Arrays for Spatial power Combining," *IEEE AP-S International Symposium*, (Atlanta, GA), pp. 466-469, June 1998
6. R.A. York, L.-Y. Chen and P. Jia, "Solid-state spatial combiner modules for TWT replacement", presented at *Workshop on Affordability and Cost Reduction for Radar Systems*, (Huntsville, Alabama), April, 2000

20000628 211

1
DTIC QUALITY INSPECTED 4

7. L.-Y. Chen, "Development of K-band spatial combiner using active array modules in an oversized rectangular waveguide", to be presented at *IMS 2000 Conference*, June, 2000
8. Pengcheng Jia, *et al.*, "Analysis of a Passive Spatial Combiner Using Tapered Slotline Array In Oversized Coaxial Waveguide", to appear at the *IEEE MTT-S International Microwave Symposium 2000*

Detailed Technical Summary

Background:

The waveguide-based system uses stacked trays of broadband traveling-wave antenna structures, housed in a metal waveguiding enclosure that is operated in the dominant TE mode. Each antenna is then essentially a waveguide-to-transmission-line transformer that couples energy from the waveguide mode to a set of power amplifier circuits. The antennas can be electrically close for high power density. Thermal management is simplified by virtue of the modular tray architecture and the surrounding metallic walls which provide a convenient heat sink. Power enters and leaves the system in a single well-defined mode and therefore power distribution and collection is simplified. Such arrays also pose a well-defined electromagnetic problem, and consequently significant progress has been made towards optimization of the structures for bandwidth and combining efficiency. The structure affords high combining efficiency, low residual phase-noise, and exhibits desirable graceful degradation characteristics. The use of standard high-volume circuit fabrication processes, a modular design, and off-the-shelf MMICs, coupled with greater reliability, should make these attractive amplifiers for cost-sensitive radar systems.

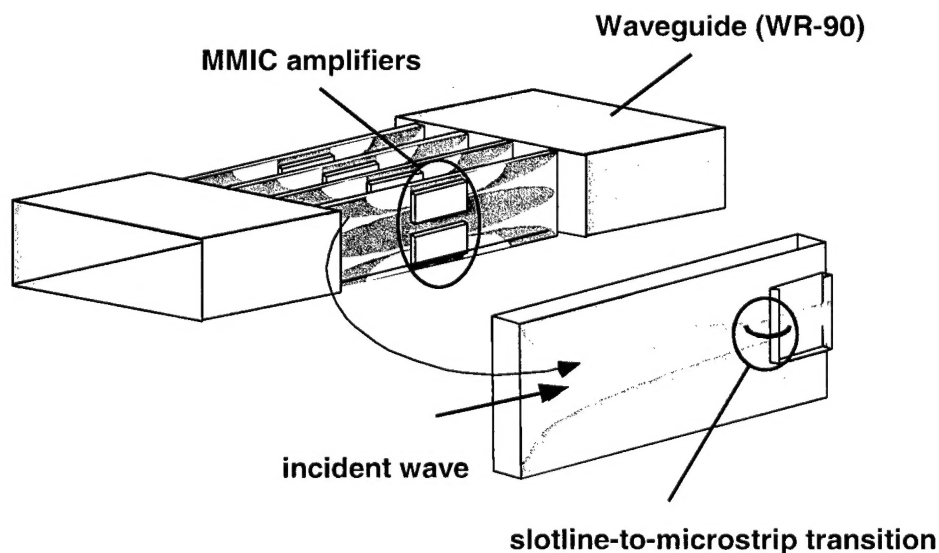


Fig. 1 — Illustration of waveguide combiner concept.

Such arrays have been successfully implemented in a "tray" architecture [1-3], as in fig. 2. The tray approach permits the use of broadband traveling-wave antennas and improved functionality through circuit integration along the direction of propagation. Each tray (fig. 1c) consists of a number of tapered-slotline or finline transitions which coupled energy to and from a rectangular waveguide aperture to a set of MMIC amplifiers. The finline transitions rest over a notched opening in the metal carrier to which the MMIC are attached. When the trays are stacked vertically, as shown in fig. 1b and 1d, the notched carriers form a rectangular waveguide aperture populated with the finline transitions. The use of the waveguide mode to distribute and collect energy to and from the set of amplifiers thus avoids loss mechanisms that would otherwise limit the efficiency in large corporate combiner structures.

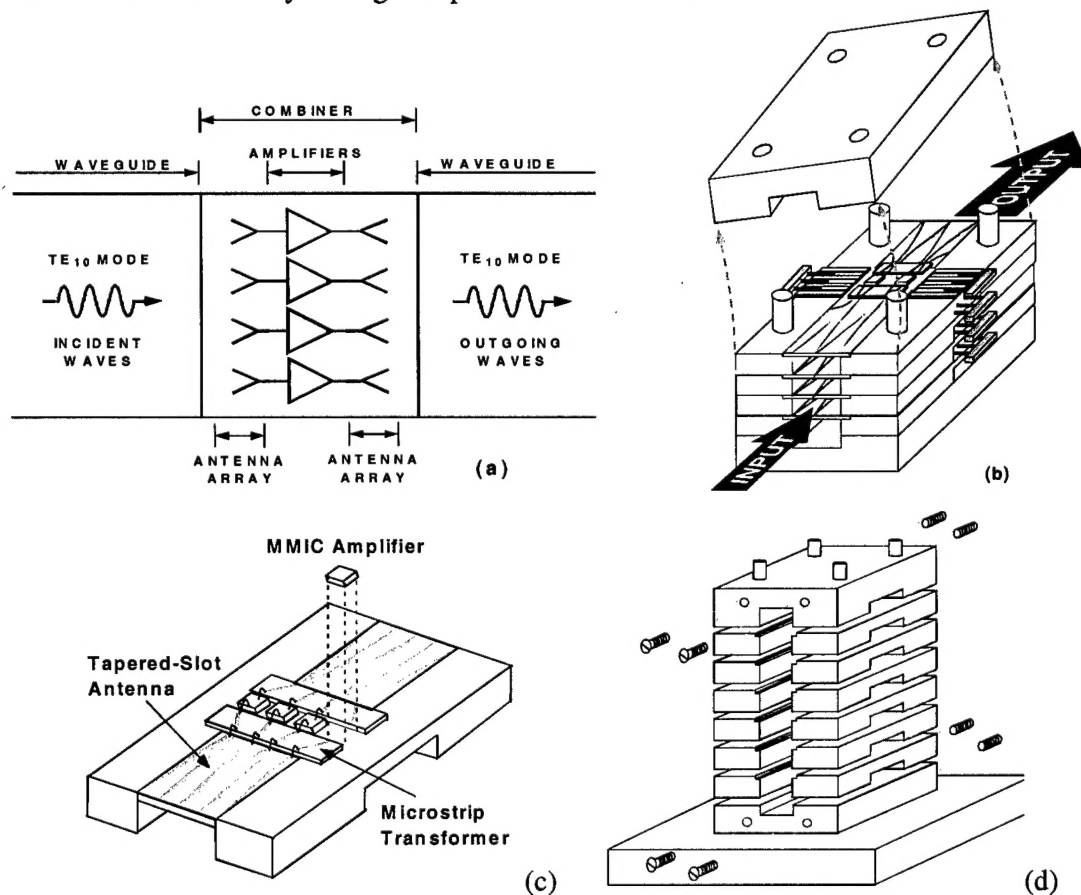


Figure 2 — (a) Schematic diagram and (b) graphical illustration of the operating principle of the combiner circuit. (c) individual tray showing finline or tapered-slot transitions and MMICs, along with microstrip interconnects. (d) Assembled system with end-caps, forming input and output waveguide apertures.

Design of the Finline Arrays

The central problem in the design of the finline combiner systems is the electromagnetic design of the tapered-slot or finline transitions. The length and shape of the taper must be chosen to provide the desired impedance level at the MMICs over the desired bandwidth, and thus determines the overall return loss of the structure.

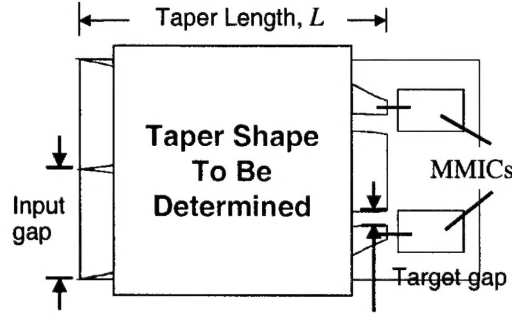


Figure 3 — Illustration of the problem statement, to determine the optimum taper shape in a multiple finline structure for matching to a set of MMICs.

The design problem is illustrated in fig.3 and can be summarized as follows: given the physical dimensions of the input and output gaps, along with the waveguide and substrate parameters, find the shape of the taper to realize a specified bandwidth and return loss. The problem is directly analogous to the synthesis of tapered transmission-line impedance transformers. From the theory of small reflections [4] it can be shown that gradual impedance taper on a non-TEM line has an input reflection coefficient

$$\Gamma_{in}(f) = \frac{1}{2} \int_0^{\theta_t} e^{-j\theta} \frac{d}{d\theta} \ln \left(\frac{Z(\theta)}{Z_0} \right) d\theta \quad (1)$$

where z is the position along the taper, L is the taper length, β is the propagation constant, and Z_0 represents the reference impedance at the input end of the taper, and

$$\theta(f, z) = \int_0^z 2\beta(f, z') dz' \quad (2)$$

is the round-trip phase delay to a point z along the taper, as shown in fig. 4. The total round-trip phase delay is $\theta_t = \theta(f, L)$.

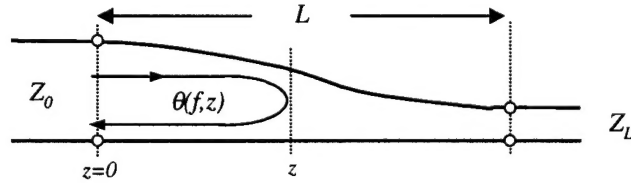


Figure 4 — Equivalent tapered transmission-line circuit for modelling the finline array.

The function $Z(\theta)$ describes the variation in impedance along the taper, and is an implicit function of z . In order to maintain an input reflection coefficient $\Gamma < \Gamma_m$ over the desired bandwidth, it has been shown [4,5] that $Z(\theta)$ must take the form

$$\ln \frac{Z(\theta)}{Z_0} = \frac{1}{2} \ln \frac{Z_L}{Z_0} + \Gamma_m A^2 F \left(\frac{2\theta}{\theta_t} - 1, A \right) \quad (3)$$

where Z_L is the terminating impedance, and

$$A = \cosh^{-1}(\Gamma_0 / \Gamma_m), \quad \Gamma_0 = \frac{1}{2} \ln(Z_L / Z_0)$$

$$F(x, A) = -F(-x, A) = \int_0^x \frac{I_1(A\sqrt{1-y^2})}{A\sqrt{1-y^2}} dy$$

and $I_1(x)$ is the modified Bessel function of the first kind and first order. The passband is defined as $\theta_i > 2A$. Assuming the propagation constant is a monotonically increasing function of frequency, the lowest operating frequency is therefore defined by

$$\theta_i(f_0) = 2A \quad (4)$$

which is an implicit relationship between the taper length L , the lower cutoff frequency f_0 , and the maximum reflection coefficient Γ_m .

The main difficulties in applying the above results to the finline arrays are the frequency dependence of the wave impedance and propagation constant, and the difficulty in translating the impedance as a function of θ into a function of z , and subsequently determining the physical parameters required to synthesize the impedance taper. The details for doing this are presented in a recent paper by the authors [11], and the reader is referred to that work for a more complete exposition of the method.

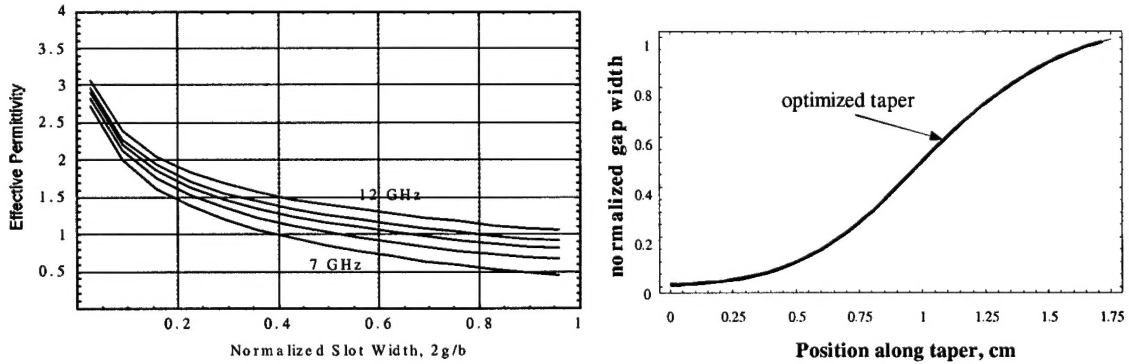


Figure 5 — (a) Effective permittivity versus normalized gap width for a 2x2 finline array in WR90 waveguide. (b) Result of optimization procedure for an optimized taper, showing the required normalized gap width vs. location along the structure.

The waveguide aperture and the number of transitions per tray determine the input gap size, but we have not yet addressed the choice of a target gap size. The target gap is determined by the desired impedance level for the MMIC amplifier. For most off-the-shelf MMICs this gap should be chosen for a 50Ω impedance. Unfortunately this is not possible in general for slotline on commonly used substrate materials. Our approach was therefore to choose the smallest realizable gap dimension, giving some impedance that is larger than 50Ω , and include a final impedance transformation to the MMIC in microstrip as part of the slot-line-to-microstrip transition.

Once the problem has been defined, the propagation constant (or effective permittivity) in the finline array is determined, and the optimum taper computed from (3). Figure 5a summarizes the

results of the propagation constant analysis for a 2-tray (4 antenna) system. Using these results, an “optimized” taper was computed for an input reflection coefficient of -20dB , shown in fig. 5b. The taper design was tested experimentally by terminating the slots in a resistive matched load, using 100Ω chip resistors as depicted in fig. 6a. Two trays were then stacked and placed centrally in a WR90 waveguide, and return loss measurements were made. The measured return loss is shown in fig. 5b, along with the theoretical predictions using the theory of sections III-IV. Excellent agreement is observed over the measured bandwidth, which was limited to 8.2-12.4 GHz due to the calibration standards used. Discrepancies between the two curves are attributed to some additional series inductance from the bonding of the chip resistors.

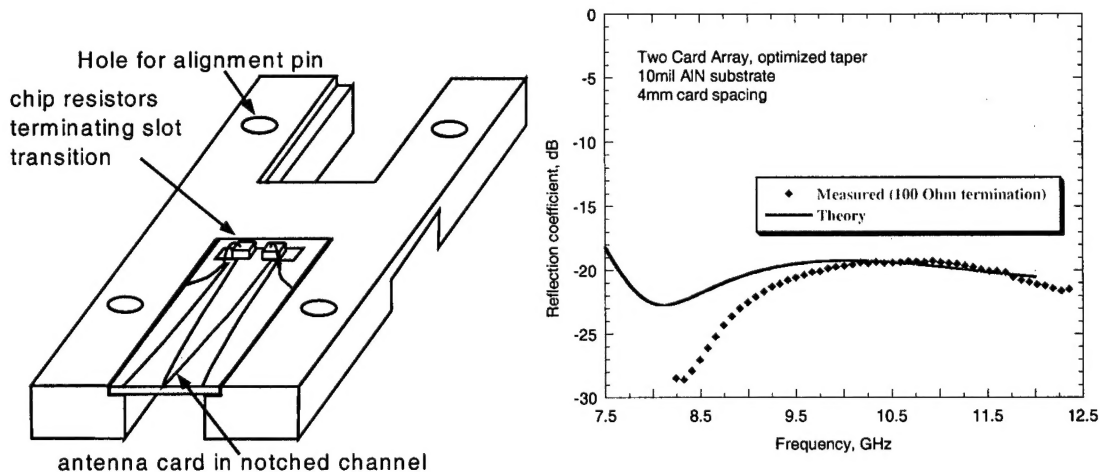


Figure 6 — (a) Finline transitions terminated in resistive loads for design verification. (b) Comparison of measured reflection coefficient with theoretical predictions for a 2x2 finline array in WR90 waveguide, using the taper design of fig. 5.

K-band Combiner Efforts

Under ARO sponsorship in this program, we attempted to build on prior successful demonstrations of the waveguide-combiner approach at X-band. This includes extending the concept to mm-wave frequencies, which requires the use of oversized waveguiding enclosures in order to accommodate a sufficiently large number of devices and trays.

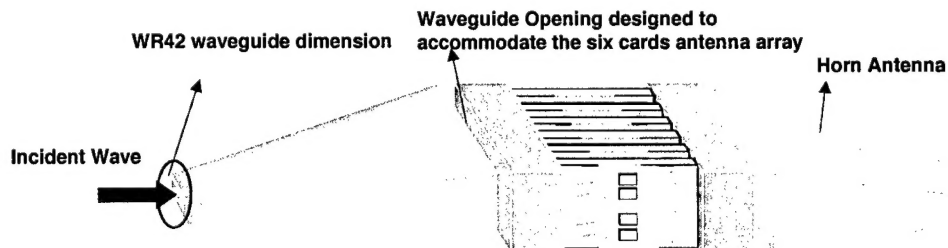


Figure 7 – Illustration of the K-band prototype oversized array system with gradual transition from standard WR-42 waveguide. The system can accommodate 24 MMICs.

Oversized Feed Structure

An oversized combiner system was design to accommodate 6 trays of active devices with 4 antennas per tray, for a total of 24 devices. Due to machining limitations, this required a waveguide aperture approximately 3 times the size of a standard K-band (WR-42) waveguide aperture. In this case both the TE₁₀ and TE₂₀ modes can propagate at the operating frequency. However, by symmetric loading of the guide, modes with odd symmetry such as the TE₂₀ mode should be effectively suppressed. A gradual transition from WR42 to the oversized waveguide was designed for testing of the system. This is illustrated in fig. 7. Using a gradual transition is necessary to suppress the excitation of high-order modes. The structure design was verified on HFSS. Measurements on the feed structure are shown in fig. 8.

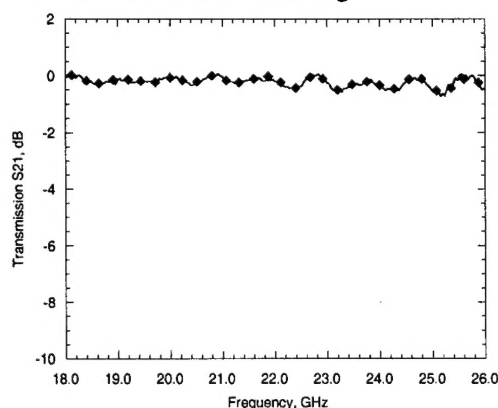


Figure 8 – Through measurement on the gradual feed structure with the passive array removed.

Slot-to-CPW Transition Design

The transition evolved from prior work at X-band, with some modifications to improve the impedance match at the finline-to-cpw interface.

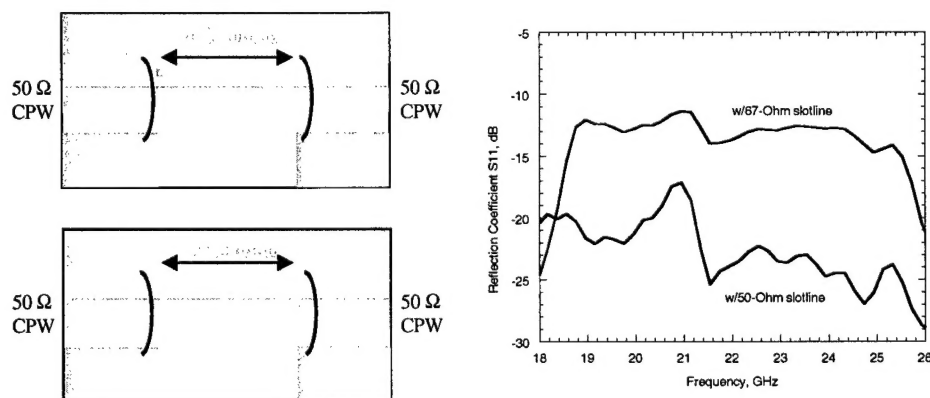


Figure 9 – Two back-to-back transitions from cpw to slotline for experimental characterization, and measurements.

In order to connect an active device to the antenna, the finline taper is gradually reduced to an asymmetrical slotline structure. In earlier work this was then connected to a microstrip line, but in this effort a coplanar waveguide transition was required. This presents a difficult

electromagnetic problem since the slot-line is a non-TEM structure and very little design information is available. Therefore HFSS simulations were critically important.

Initially it was thought that the slot-line should be design to match the gap of a 50Ω cpw line, to minimize reflections arising from abrupt changes in the transmission-line cross section. This required a 67Ω slotline structure as shown in fig. 9. However, subsequent simulations suggested that the impedance mismatch was more severe than the abrupt change in cross, section, and so a second transition was investigated using 50Ω slotline. Measured results shown in fig. 9 confirmed the simulations and showed that an excellent match could be achieved.

Antennas and Characterization

The final step in the passive array development involved the integration of a tapered-slot or finline antenna with the slot-to-cpw transitions, and characterization of the structures in the waveguide environment with 50Ω terminations to simulate the active circuit. The final antenna cards are shown in figure 10, along with a photo of one card in its tray fixture.

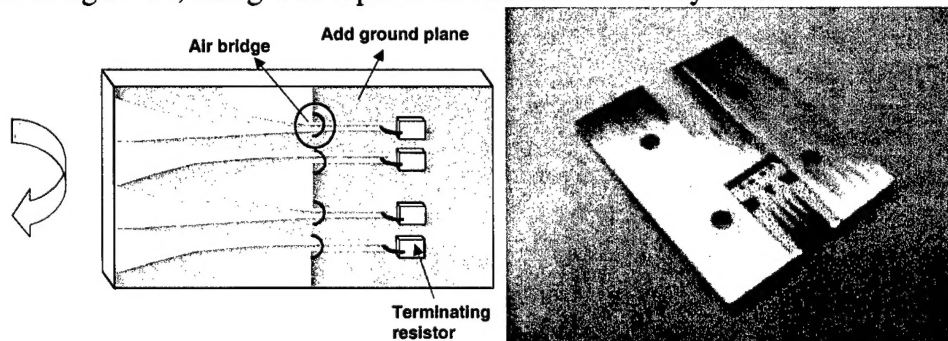


Figure 10 – Illustration of the antenna card shown 4 tapered-slot or finline antennas, which gradually transition from the waveguide aperture to a slotline and then to a cpw-line, which is terminated in a 50Ω chip resistor.

Array Module and Test Fixture

A machined test fixture including 6 trays of the type shown in figure 10, as well as the gradual taper from standard to oversized waveguide, was constructed from Aluminum. Individual trays were aligned with vertical pins. Each tray included provision for lateral insertion of biasing wires for addition of active device later in this program. The completed waveguide system is shown in figure 11a. Measurements on the passive structure with a 6×4 array of terminated finline antennas is shown in fig. 11b, suggested good low-loss and broadband characteristics in the desired operating band. This initial design is a linearly scaled version of the X-band passive system reported under DARPA MAFET sponsorship.

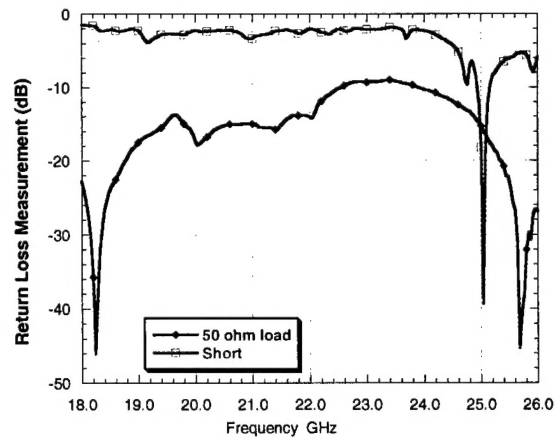
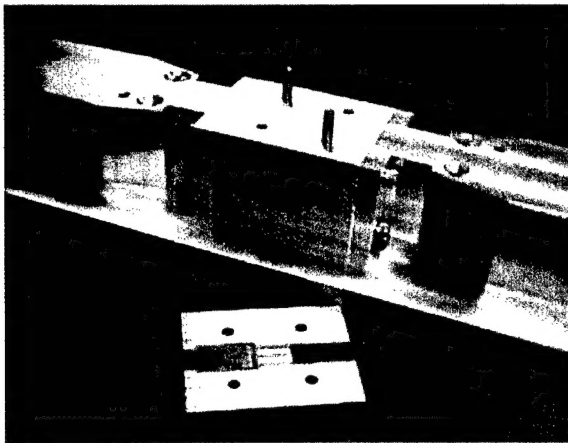


Figure 11 – (a) Photo of 6-tray K-band (18-20GHz) combiner prototype. (b) Measured data on the passive structure with terminated finline arrays.....

The return loss measurements with terminated finline arrays is a good measure of the impedance matching behavior of the antennas, but does not give any indication of the losses in the system which is relevant to combiner efficiency. Therefore, a second set of measurements was performed using input and output finline arrays coupled by a through line (in place of a MMIC amplifier). These measurements are shown in figure 12 for 2,4, and 6 trays of 4 antennas per tray.

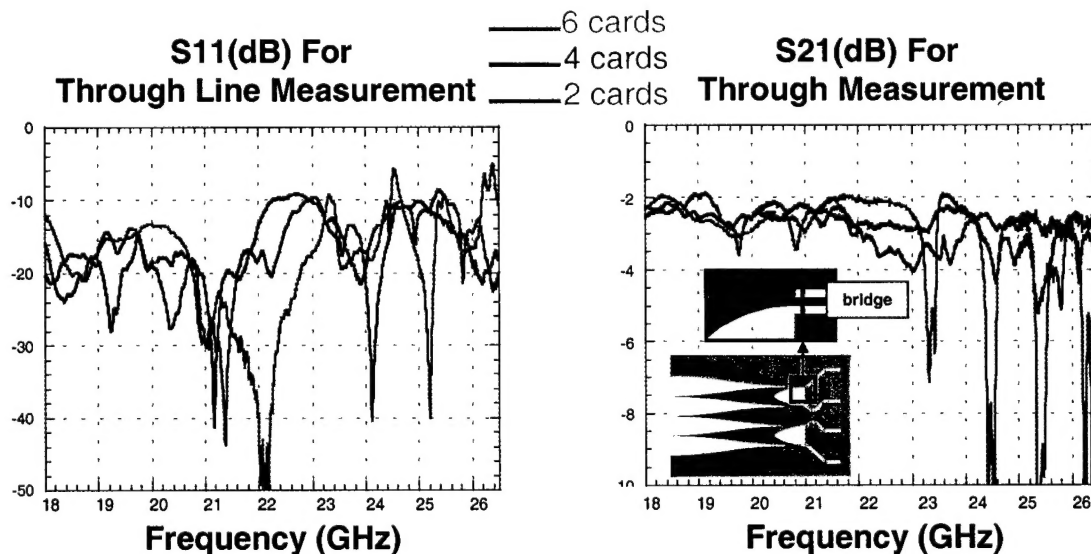


Figure 12 – Measurements on the passive combiner system using a through-line between input and output antennas.

The losses in the band of interest are between 2-2.5dB, corresponding to an output loss of 1-1.25dB. The combining efficiency computed from these measurements is shown in figure 13. This is the maximum possible combining efficiency that the structure will support, limited by ohmic and mode-coupling losses in the passive structure.

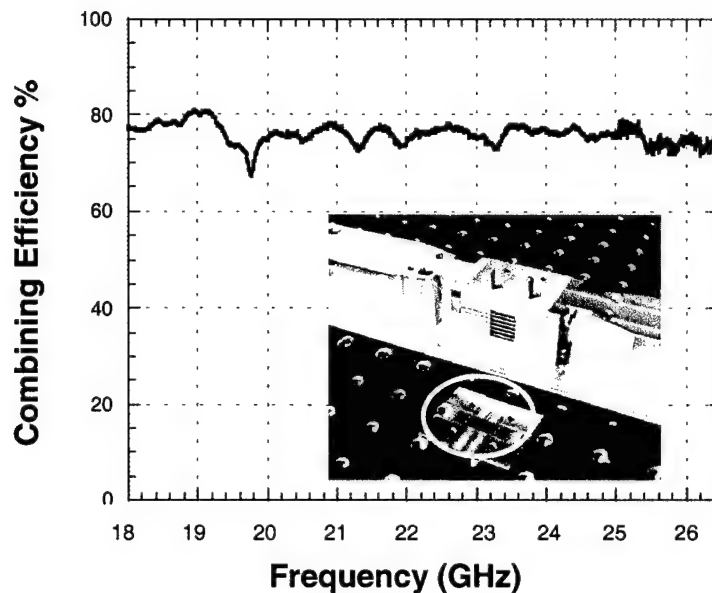


Figure 13 – Maximum possible combining efficiency computed from insertion loss measurements.

Flip-Chip Amplifier Technology

UCSB developed a hybrid flip-chip amplifier technology for K-band amplifiers using commercial off-the-shelf (COTS) discrete devices for use in these combiner systems. In this technology a COTS device is flip-chip bonded to an AlN carrier using thermal-compression bonding to a set of raised gold “bumps” patterned into the appropriate device footprint. The AlN substrate carries all additional circuitry including cpw transmission-line, thin-film resistors and capacitors, etc. A simple one-stage amplifier design is shown in fig. 14a (inset) along with measured small signal data. Data comparing multiple amplifiers in this design are shown in fig 14b, indicating that reproducible characteristics can be achieved with this technology.

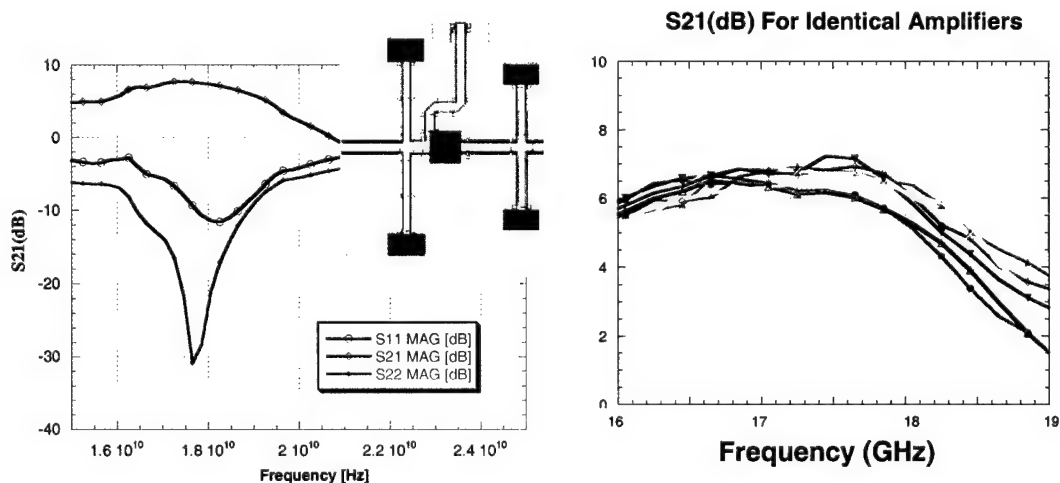


Figure 14 – (a) Measured small-signal performance of an K-band amplifier using flip-chip mounted commercial pHEMT on an AlN carrier. (b) Single tray for K-band system using 4 amplifiers per tray.

Fig. 15a compares the measured power and gain data versus the simulation, showing reasonably good agreement. An initial tray design based on the flip-chip amplifier of fig 14 is shown in fig. 15b, with 4 amplifiers per tray.

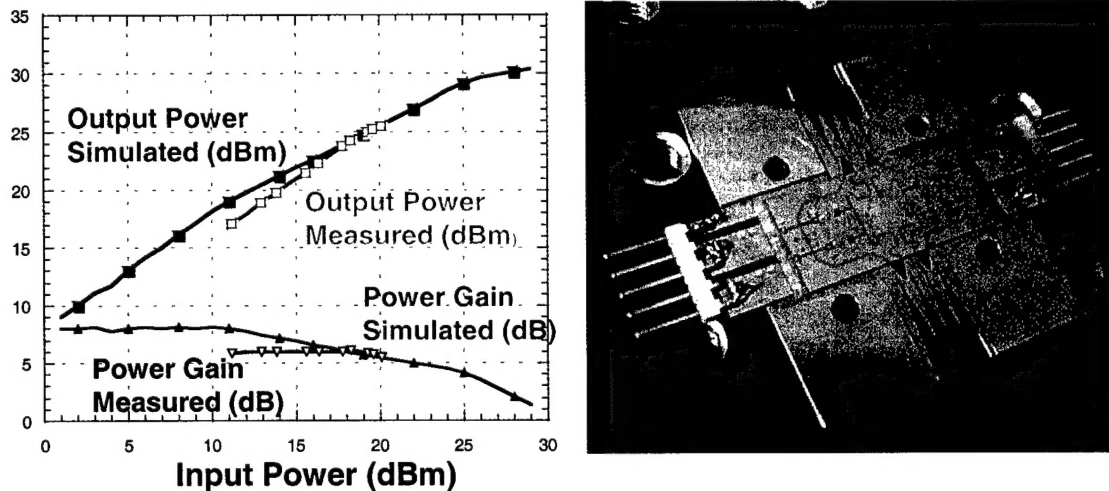


Figure 15 – (a) Measured small-signal performance of an K-band amplifier using flip-chip mounted commercial pHEMT on an AlN carrier. (b) Single tray for K-band system using 4 amplifiers per tray.

Initial measurements on the active system using the tray design of fig. 15b were disappointing. This was ultimately traced to a poor wirebond connection between the antenna cards and the amplifier trays. Subsequently these cards were redesigned and integrated together to eliminate this wirebond entirely. This design is shown below. UCSB is currently testing this array design, and results will be reported in future publications.

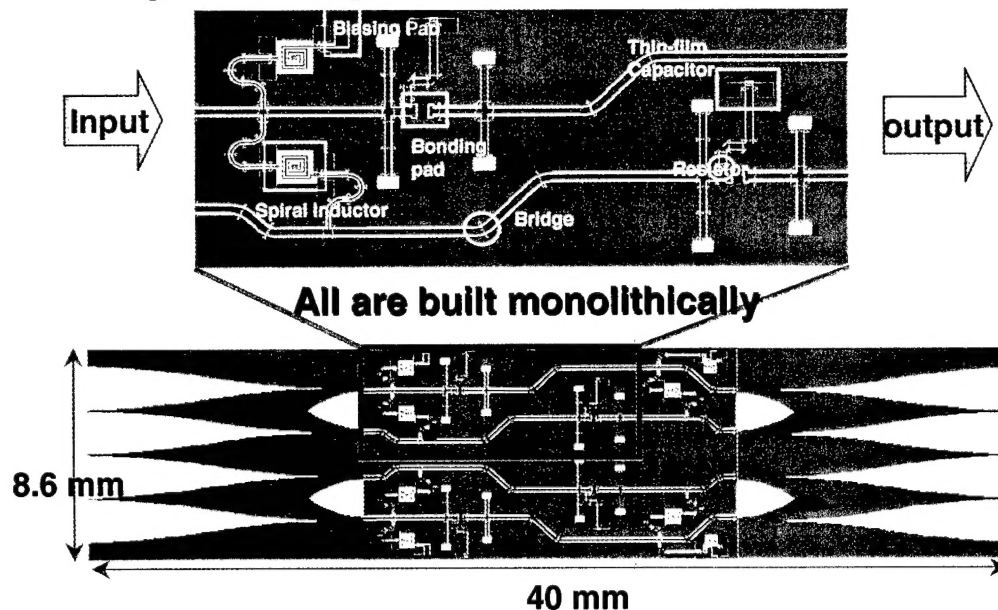


Figure 16 – Redesigned K-band tray with 4 flip-chip amplifiers and antennas on a single AlN substrate.

Coaxial Combiner Structure

UCSB is also investigating topologies which can be used to greatly increase the bandwidth and number of devices. One attractive possibility is shown in fig. 17, which is a coaxial waveguide-based combiner system. The use of a TEM-mode combiner means that there is no cutoff frequency for the structure, providing a much wider operating band. In addition, the perfect rotational symmetry of the structure greatly simplifies the modeling, since the array analysis can be reduced to the analysis of a single unit cell with appropriate floquet boundary conditions.

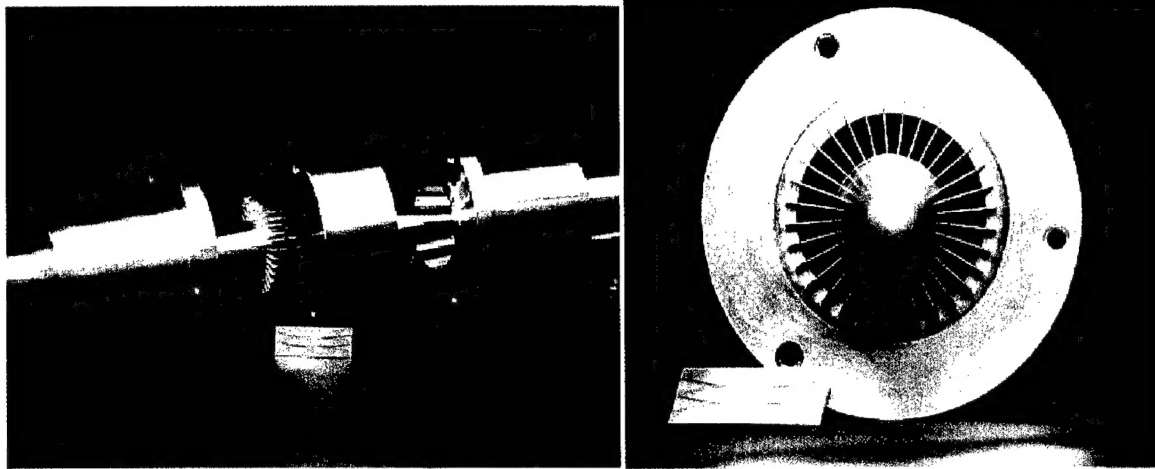


Figure 17 – (a) Exploded view of coaxial combiner. (b) Axial view of center section with finline cards.

Initial theoretical and experimental efforts on the prototype of fig. 17 are summarized in fig. 18, showing insertion loss and return loss for a 32-card (64-way) combiner. The system is capable of operation from 4-20GHz with excellent broadband matching and low loss, and the measured results compare favorably with modeling efforts. Currently UCSB is attempting to implement an active version of this combiner using a combination of GaAs pre-amplifiers and GaN-based power-amplifiers.

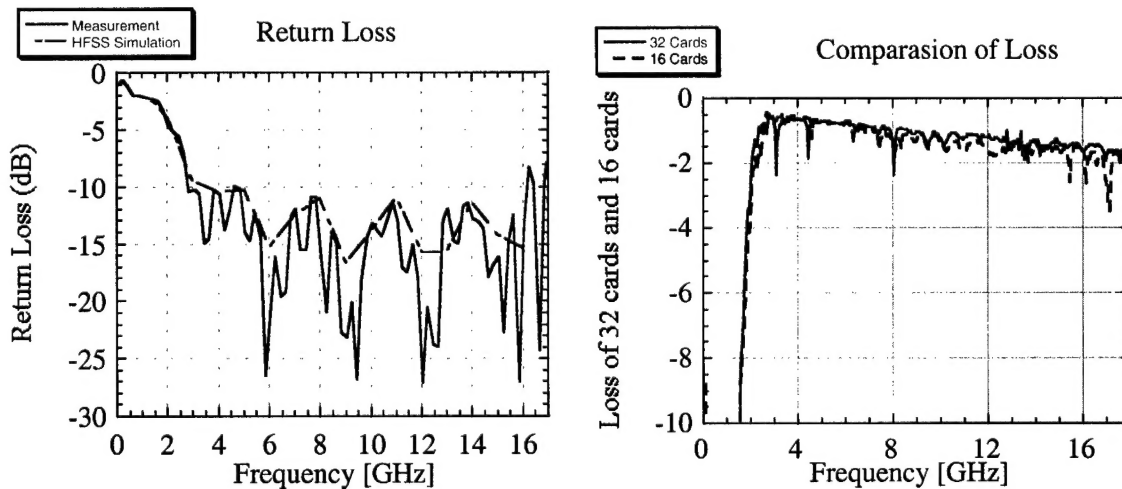


Figure 18 – (a) Return loss and (b) insertion loss for the coaxial combiner.

Conclusions

Exciting progress has been made in the development of high-power solid-state amplifiers using a spatial combining approach within an enclosed waveguide structure. The combiners presented herein have demonstrated high output power and combining efficient with broadband performance. The combiners exhibit graceful degradation, and the modular design provides for convenient fabrication and manufacture. The excellent heat-sinking capacity of the combiner has been verified during power measurements, with as much as 415 Watts of DC power dissipated by the MMIC amplifiers in one design. The approach provides a broadband impedance match to the MMICS and is transparent to the device technology. The results so far have been encouraging, suggesting a promising outlook for our combining system to compete with the currently dominating traveling-wave tube amplifiers (TWTAs) in high-power applications.

References for the Technical Report

1. N.-S. Cheng, "Waveguide-Based Spatial Power Combiners", Ph.D. Dissertation (ECE Technical Report #99-08), Dept. of Electrical and Computer Engineering, University of California, Santa Barbara CA, 93106, June 1999.
2. A. Alexanian and R.A. York, "Broadband Spatially Combined Amplifier Array using Tapered Slot Transitions in Waveguide", *IEEE Microwave Guided Wave Lett.*, vol. 7, no. 2, pp. 42-44, Feb 1997
3. N.-S. Cheng, A. Alexanian, M. G. Case, D. B. Rensch and R. A. York, "40 Watt CW Broadband Spatial Power Combiner Using Dense Finline Arrays", *IEEE Transactions on Microwave Theory and Techniques*, vol. 47, no. 7, July 1999.
4. D. M. Pozar, *Microwave Engineering*, 2nd Ed., New York, NY: John Wiley & Sons, 1998.
5. R.W. Klopfenstein, "A Transmission-Line Taper of Improved Design," *Proc. IRE*, vol. 442, pp. 31-35, January 1956.
6. Schieblich, J.K. Piotrowski, J.H. Hinken, "Synthesis of Optimum Finline Tapers using Dispersion Formulas for Arbitrary Slot Widths and Locations", *IEEE Trans. Microwave Theory Tech.*, vol. MTT-32, pp. 1638-1644, Dec 1984.
7. C.Verver and W. Hoefer, "Quarter-wave matching of waveguide-to-finline transitions", *IEEE Trans. Microwave Theory Tech.*, vol. MTT-32, pp. 1645-1648, Dec. 1984.
8. L.P. Schmidt and T. Itoh, "Spectral Domain Analysis of Dominant and Higher Order Modes in Fin-lines", *IEEE Trans. Microwave Theory Tech.*, vol. MTT-28, pp. 981-985, Sept 1980
9. T. Itoh, "Spectral Domain Immitance Approach for Dispersion Characteristics of Generalized Printed Transmission Lines", *IEEE Trans. Microwave Theory Tech.*, vol. MTT-28, pp. 733-737, July 1980.
10. N.-S. Cheng, P. Jia, D. B. Rensch and R. A. York, "A 120-Watt X-Band Spatially Combined Solid-State Amplifier", *IEEE Trans. Microwave Theory Tech.*, Dec 1999.
11. P. Jia, L-Y Chen, N-S. Cheng, and R.A. York, "Design of Waveguide Finline arrays for Spatial Power Combining", submitted to *IEEE Trans. Microwave Theory Tech.*, Feb 2000.
12. Pengcheng Jia, *et al.*, "Analysis of a Passive Spatial Combiner Using Tapered Slotline Array In Oversized Coaxial Waveguide", to appear at the *IEEE MTT-S International Microwave Symposium 2000*

Scientific Personnel supported by this project:

Robert A. York and Lee-Yin Chen

Inventions:

N/A